Structure and Properties of Rubber-Modified Polypropylene Impact Blends

FERDINAND C. STEHLING, TERRY HUFF, C. STANLEY SPEED, and G. WISSLER, *Plastics Technology Division, Exxon Chemical Company, Baytown, Texas 77520*

Synopsis

The state of dispersion of poly(ethylene-co-propylene) (PEP) rubber and high-density polyethylene (HDPE) in polypropylene (PP) blends was investigated using scanning electron microscopy to examine solvent-etched microtomed surfaces cut at low temperatures. The validity of the method was established by comparing the areal fraction of dispersed particles in micrographs with the volume fraction of PEP and HDPE in PP-rich blends. When small amounts of PEP and HDPE were added to PP, they combined to form composite PEP–HDPE particles with characteristic internal structures in a PP matrix. Changes in impact strength and flexural modulus with changes in mixing conditions and blend composition were determined and interpreted in terms of the size, composition, and internal structure of the dispersed particles. Particle growth in the melt limited the impact strength level achieved in molded articles. A simple model proposed for screening rubbers for toughening of brittle plastics successfully predicts that PEP rubber should be an excellent impact modifier for PP.

INTRODUCTION

The poor impact strength of polypropylene (PP) at low temperatures is a deficiency of this plastic in some applications. Its toughness can be improved by incorporating rubber into the plastic by blending or by *in situ* polymerization of the rubbery component. Poly(ethylene-co-propylene) (PEP) is widely used in commercial impact PP resins. Although rubber addition improves impact strength, it causes a decrease in flexural modulus. The magnitude of the modulus decrease can be minimized by also introducing high-density polyethylene (HDPE) into the system. A knowledge of the morphology of toughened PP would be helpful in understanding and further improving the properties of impact-grade PP. However, only a few morphologic studies of toughened PP have been reported. The main purpose of our work was to develop and apply a reliable method for examining the morphology of such systems.

Methods for examining the morphology of rubber-toughened plastics and the influence of morphology on mechanical properties have been critically reviewed by Bucknall.[2] Optical microscopy has limited application in morphological investigations because of the low resolution, about 0.5 μm, of optical techniques. When one of the components of a blend is unsaturated, as in terpolymers of acrylonitrile, butadiene, and styrene, then the morphology can be clearly seen by Kato's method using osmium tetroxide-stained thin sections viewed by transmission electron microscopy (TEM).[3–5] This technique, among others, was applied by Thamm[6] and Speri and Patrick[7] to binary PP–EPDM (ethylene–propylene–diene terpolymer) blends and ternary PP–EPDM–HDPE blends. In binary blends containing EPDM as the minor component, the rubber was

Journal of Applied Polymer Science, Vol. 26, 2693–2711 (1981)
 CCC 0021-8995/81/082693-19$01.90

particulately dispersed into particles as small as 0.05 μm. In PP-rich blends containing both HDPE and EPDM, unstained areas were found within the EPDM regions. These unstained areas included within EPDM regions were assumed to consist of HDPE.

Although TEM observation of stained thin sections is a powerful technique for examining morphology of polymer mixtures, it suffers several disadvantages. It requires considerable skill in ultramicrotomy to cut suitable thin sections. More fundamentally, the method is not applicable to systems composed of saturated polymers that cannot be selectively stained, such as PP–PEP blends and PP–PEP–HDPE blends.

Scanning electron microscopy (SEM) does not suffer these limitations. Surfaces for SEM examination have usually been obtained by fracturing the sample. The fracture surfaces have been examined directly, or after removal of the rubbery component therefrom by selective oxidative attack or solvent leaching. Conceivable disadvantages of this technique are: (1) the state of rubber dispersion on the fracture surface is not necessarily representative of the dispersion in the bulk specimen, and (2) the oxidative attack or solvent leaching may introduce artifacts. However, Salovey, Naderi, and Chompff[8] used SEM to examine hexane-extracted fracture surfaces of PP–EPDM and PP–EPDM–HDPE blends and found morphological features similar to those reported by Thamm[6] and Speri and Patrick.[7]

Surfaces for SEM examination can also be obtained by microtomy. If it were assumed that a cut through the specimen were equivalent to passing a plane through the specimen, then a microtomed surface, after oxidative or solvent treatment to remove rubber, should provide a more representative view of the bulk structure of the composite than a fracture surface. Salovey et al. examined microtomed surfaces obtained by cutting frozen PP–PEP blends, but they reported that morphological details were always distorted by the cutting action.[8]

The main objective of our work was to develop a quantitative method for determining the state of dispersion existing in binary PP–PEP and ternary PP–PEP–HDPE blends containing small concentrations (5–20%) of PEP and HDPE. Our method, which is based on the SEM examination of solvent-extracted surfaces microtomed at low temperatures, and its applications to the understanding of the impact strength and modulus of PP-rich impact blends are described below. We also suggest a simple model for use as a guide in selecting a rubber for toughening a brittle plastic.

EXPERIMENTAL

Materials

Polypropylene used in this work was Exxon Chemical Co. grade E115 with a 5.0 melt flow rate measured by ASTM D1238L. High-density polyethylene used was Allied Chemical Co. grade AA60003 with density 0.960 g/cm^3 and a 0.3 melt index measured by ASTM D1238E. The PEP used was Exxon Chemical Co. Vistalon 404, with a Mooney viscosity of 40 (1 + 8′ at 100°C) measured by ASTM D1646, containing 40 wt % ethylene.

Blending

Blends were prepared by a number of different methods in order to vary the state of dispersion of the components of the system. Some blends were made using a Banbury batch mixer, whereas others were made in a Farrel Continuous Mixer. Severity of mixing in these intensive mixing devices was varied by changing melt temperature and melt residence times. Certain of the blends were prepared in a two-stage process in which a PEP–HDPE blend made in a Farrel Continuous Mixer was mixed with PP in an extruder. The severity of mixing in the extruder was varied by changing melt temperatures, screen pack mesh sizes, and extruder back pressure.

The composition of blends is expressed in weight percent unless stated otherwise. Thus, an 80PP–10PEP–10HDPE mixture contains 80, 10, and 10% by weight PP, PEP, and HDPE, respectively. In cases where volume percent concentrations are given, these were calculated from weight concentrations assuming densities of PP, PEP, and HDPE equal to 0.91, 0.85, and 0.96 g/cm^3, respectively.

Molding and Mechanical Testing

Compression-molded samples for morphological examination and mechanical testing were made in a press at a 200°C melt temperature, generally with 5 min of melt residence time, followed by cooling between room-temperature platens. Injection-molded samples were prepared using a molding machine equipped with a reciproscrew feed. Flexural modulus values were measured following ASTM D790. Izod impact strength was determined using ASTM D256. However, in some Izod impact strength tests the specimens were not notched. Falling weight impact strength (ASTM D3029) was determined on 2.3-mm-thick injection-molded samples.

Surface Preparation and SEM Conditions

An ultramicrotome, LKB Ultratome III 8800 with low-temperature LKB 14800 Cryokit and glass knives made with the LKB 7800 Knife Maker, was used to cut surfaces for observation. Surfaces cut at room temperature were invariably distorted by the cutting action, as were surfaces cut at lower temperatures with a dull knife. However, surfaces that appeared undistorted and smooth when viewed in an SEM at 20,000× magnification were consistently obtained at the following cutting conditions: knife edge condition, freshly cut with no visible flaws when examined at 50× magnification; knife angle, 48°; knife clearance angle, 7°; knife temperature, −120°C; sample temperature, −140°C; and sample cross section, ~0.5 × 1 mm. The glass knife was quickly dulled in low-temperature cutting operations, so a fresh length of knife edge was used to cut each surface. To compare fracture and microtome surfaces, some samples were fractured at −196°C.

Etching with xylene selectively dissolved PEP from the cut surface, leaving PP and HDPE undissolved. Surfaces were generally etched in xylene in a thermostatted ultrasonic bath at 25°C for 9 min. Changing etching time over the range from 1 to 120 min showed no difference in SEM micrographs of the surface. Surfaces etched in an ultrasonic bath were also indistinguishable from

those etched with a laboratory shaker from 1 to 24 h. A few samples were etched with chromic acid for several hours at 50–60°C. However, structural details could be more clearly discerned on xylene-etched samples, and acid-etched surfaces are not discussed further in this report.

The etched surfaces were examined using mainly an AMR 1000 SEM after coating with gold–palladium alloy. Micrographs were obtained by collecting secondary electrons emitted upon bombarding the sample with 10 kV electrons. The incident electron beam was perpendicular to the surface to prevent geometric distortions in the micrographs. Micrographs were obtained at magnifications ranging from 1000 to 20,000.

Micrograph Analysis

Micrographs of etched surfaces showed circular depressions similar to those seen in the PP–PEP blend in Figure 1(a) and PP–PEP–HDPE blend in Figure 1(c). Such micrographs were analyzed to obtain the areal percent dispersed phase and various moments of the particle diameter distribution. The areal percent dispersed phase was found by preparing a transparent rectangular grid having approximately 7000 points with a spacing corresponding to 0.25 μm (at 5000×, the magnification most suitable for analyses). The grid was placed on the micrograph and the fraction of grid points falling within the boundaries of the circles was determined by manual counting. The areal percent dispersed phase could be determined by different analysts to a precision of ~1% (absolute) on a given micrograph. Because of local variations in rubber concentration and because of the small region viewed in each micrograph, it was necessary to analyze a number of micrographs obtained from several cuts of a sample to obtain representative results.

Cutting compression-molded samples in various directions and at various locations in the specimens showed that the particles were closely spherical and that the concentration of particles did not vary systematically over the specimen. However, particles close to the surface of injection-molded samples were nonspherical. Determination of the particle size of injection-molded specimens was restricted to the central region of the samples where the dispersed particles were closely spherical.

RESULTS AND DISCUSSION

In the following discussion, we first examine the disperse phase structure of binary PP–PEP systems. We then consider the structure of ternary PP–PEP–HDPE blends and the effect of structure on impact strength and modulus of such blends. Finally, we present a simple theory that explains why PEP is an excellent rubber for toughening PP.

Morphology and Properties of Binary PP–PEP Blends

The validity of our method for examining the structure of binary PP–PEP blends was established from the examination of a series of blends of known composition. As illustrated in Figure 1(a), solvent-etched surfaces of such samples show circular depressions where PEP originally resided. If PEP were

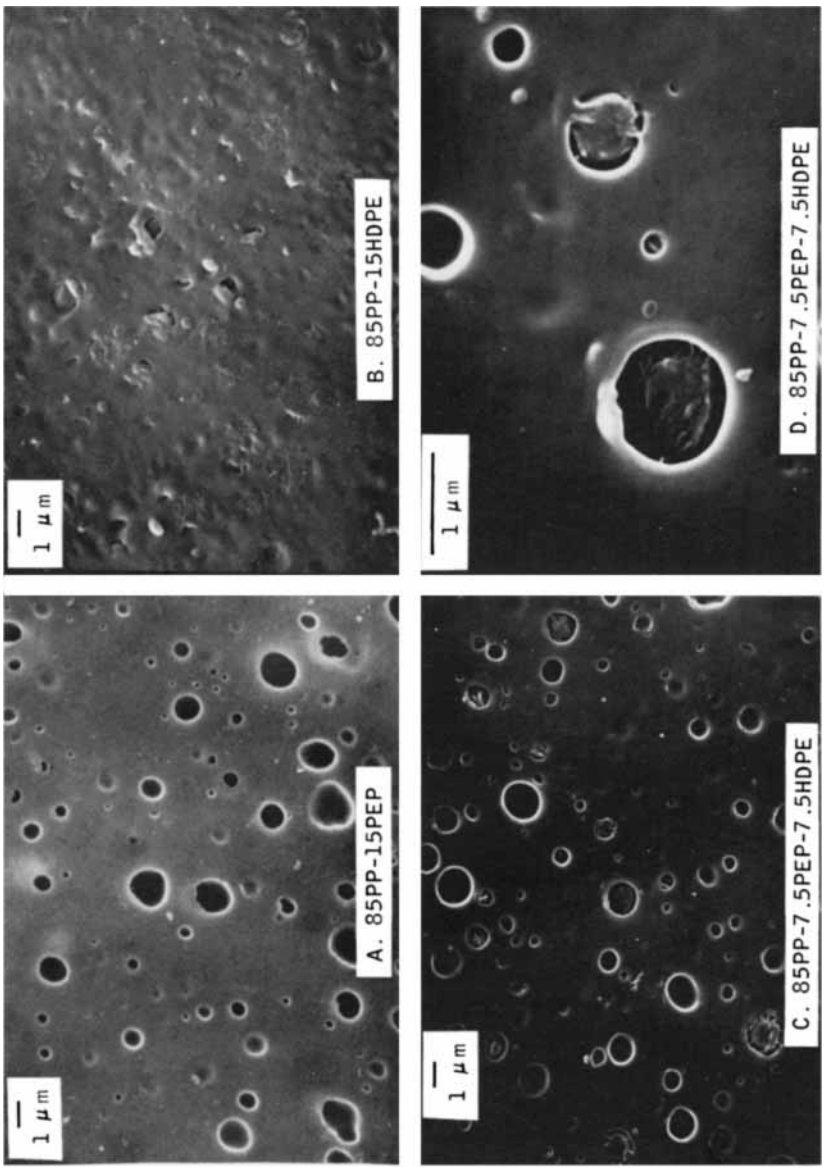

Fig. 1. Scanning electron micrographs of xylene-extracted microtomed surfaces from binary and ternary blends: (a) compression-molded 85-PP–15PEP sample made from intensively mixed blend; (b) compression-molded 85PP–15HDPE sample made from intensively mixed blend; (c) compression-molded 85PP–7.5PEP–7.5HDPE sample made from intensively mixed 50:50 blend of 85PP–15PEP and 85PP–15HDPE; (d) higher-magnification micrograph of partially filled holes in 85PP–7.5PEP–7.5HDPE blend.

insoluble in PP, if the dispersed PEP contained no PP inclusions, and if our method were completely accurate, then the areal fraction of the holes seen in the micrographs should exactly equal the volume fraction of rubber in the blend. Areal fraction vs. volume fraction of PEP is plotted in Figure 2 for blends containing from 5 to 20% PEP. The number in parentheses next to each point is the number of micrographs that was analyzed and averaged for that point. The indicated error represents one standard deviation. The solid line in the figure is the "areal fraction = volume fraction" locus. To an excellent approximation, the experimental points fall on this locus. These results show that PEP is almost completely insoluble in PP at room temperature and that our method provides an unbiased, representative view of the bulk morphology of such blends. The sizable standard deviation of the areal fraction is caused by local variations in composition, and a number of micrographs for each sample must be analyzed to obtain accurate results. Using stained thin sections of PP–EPDM blends viewed by transmission electron microscopy, Thamm has shown that very small quantities of PP are sometimes occluded within EPDM particles.[6] Small quantities of occlusions, less than ~1%, would not be detected by our method.

Because our method provides accurate estimates of the rubber content of binary blends, it is reasonable to assume that particle size estimates obtained from the micrographs are also accurate. Of course, it should be recognized that the distribution of section diameters seen on a cut surface differs from the distribution of particle diameters in the sample. For example, if monodisperse particles with diameter d_0 are cut at random, then a distribution of section diameters ranging from 0 to d_0 is obtained. For spherical particles having an arbitrary size distribution, the particle diameter distribution can be obtained from the distribution of section diameters by a suitable mathematical treatment. Additionally, various moments of the particle diameter distribution can be calculated from measured section diameter moments using published formulae.[9] In our work, section diameters were measured manually from micrographs. First,

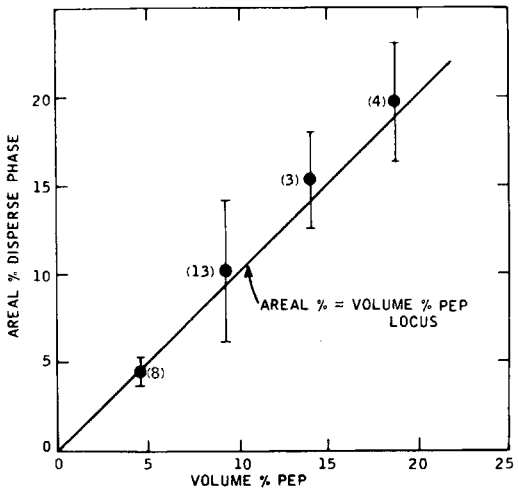

Fig. 2. Areal percent disperse phase in scanning electron micrographs of compression-molded PP–PEP blends having various compositions.

second, and third moments were computed, and they were multiplied by 1.31, 1.50, and 1.69, respectively, to obtain the first, second, and third moments of the particle diameter distribution $\bar{d}_1$, $\bar{d}_2$, and $\bar{d}_3$, respectively.[9]

The variation of impact strength attendant with changes in particle size is illustrated for 80PP–20PEP blends in Table I. The relatively well-dispersed sample, blend 1, had substantially better low-temperature impact strength than the poorly dispersed sample, blend 2. The toughness of the poorly dispersed sample is only modestly greater than that of pure PP, whose −18°C unnotched Izod impact strength and −18°C falling weight impact strength are 2.6 J/cm and 0.3 J, respectively. Our results on the effect of particle size on impact strength are consistent with those of Speri and Patrick, who varied particle size in PP–EPDM blends by changing the molecular weight of PP.[7] It has been shown by Karger-Kocsis et al.[10] that incorporation of PEP into PP causes a change in the superstructure of the PP matrix. Consequently, morphological factors other than rubber dispersion may contribute to the differences in impact strength noted in Table I.

Comparison of data obtained from microtome surfaces and fracture surfaces show that incorrect conclusions about the bulk morphology of blends may be drawn from the examination of fracture surfaces. A blend containing 14.2 vol % PEP in PP was compression molded into Izod impact test bars. The etched microtomed surfaces from such bars gave 15.1 ± 2.7% disperse phase, a value which agrees with the rubber content of the blend. In addition, test bars were notched, cooled to −196°C, and broken in an Izod impact tester. The etched fracture surface was examined at three locations—close to the region of crack initiation, at an intermediate location, and at a remote location from the initiation site. The areal percent dispersed phase in these regions was 10.3 ± 1.2, 8.7 ± 0.9, and 4.7 ± 1.7%, respectively. Thus, the concentration of rubber particles on the fracture surface was less than the bulk concentration, indicating that the propagating crack tended to pass through the PP matrix rather than through the frozen rubber particles. Section diameters on fracture surfaces were not quantitatively analyzed. These results suggest that information pertaining to

TABLE I
Comparison of Particle Size[a] and Impact Strength of Injection-Molded Blends

80 PP-20 PEP Blends	Blend 1	Blend 2
Diameter moments, μm		
$\bar{d}_1$	1.2	1.4
$\bar{d}_2$	1.7	2.4
$\bar{d}_3$	2.4	3.7
Izod impact strength at −18°C, unnotched, J/cm	6.4	4.8
Falling-weight impact strength at −18°C, J	9.6	5.4
80 PP-10.7 PEP—9.3 HDPE Blends	**Blend 3**	**Blend 4**
Diameter moments, μm		
$\bar{d}_1$	0.64	2.1
$\bar{d}_2$	0.95	4.4
$\bar{d}_3$	1.7	6.5
Izod impact strength at −18°C, unnotched, J/cm	16	7.5
Falling-weight impact strength at −18°C, J	11.1	5.8

[a] The indicated particle diameters were obtained on injection-molded Izod impact test pieces. Particle diameters on falling-weight impact test pieces were not measured.

fracture mechanisms could be obtained by a comparison of rubber content and particle size distribution on fracture and microtome surfaces.

Morphology of Ternary PP–PEP–HDPE Blends

The experiments described below show that PP, PEP, and HDPE are essentially insoluble in each other at room temperature. Nevertheless, PEP and HDPE have an affinity for each other, and they tend to combine within PP to form a characteristic morphology with HDPE particles surrounded by a rubber shell. These composite PEP–HDPE particles are unstable and grow in the melt.

The affinity between PEP and HDPE in PP is illustrated by the following experiments. Figure 1(c) is a micrograph of an 85PP–7.5PEP–7.5HDPE blend prepared by mixing an 85PP–15PEP and an 85PP–15HDPE blend in equal proportions. The micrograph of the ternary blend contrasts sharply with micrographs of the PP–PEP and PP–HDPE blends [Figs. 1(a) and 1(b), respectively] from which the ternary blend was prepared. Contrary to what might be expected, it is apparent that ternary blends do not consist of rubber particles and HDPE particles separately imbedded in PP. Rather, there are both empty holes and partly filled holes in the micrograph of the ternary blend. A larger magnification micrograph of typical partly filled holes, Figure 1(d), shows a dense residue with some attachments to the matrix. Other PP-rich ternary blends mixed under many different conditions showed similar features. Departure from this characteristic morphology was observed only when the PEP and HDPE were preblended before mixing with PP (see below).

The source of the features seen in ternary blend micrographs such as those in Figure 1(c) was determined from quantitative measurements of the area of the dispersed phase in ternary blends having various compositions. The areal fraction of dispersed phase was determined by summing the area occupied by empty holes and partly filled holes. The results for 80PP–10PEP–10HDPE, 85PP–7.5PEP–7.5HDPE, and 90-PP–5PEP–5HDPE blends are given in Figure 3. Here, the areal fraction of disperse phase is plotted against the sum of the volume fractions of PEP and HDPE. The solid line in the figure is the "areal fraction = sum of volume fractions" locus. It is apparent from the proximity of the points to the solid line that the areal fraction disperse phase closely equals the sum of the PEP and HDPE volume fractions. Thus, HDPE and PEP have combined to form the dispersed phase. The residues in the partly filled holes seen in Figure 1(c) are therefore identified as HDPE particles that were partially surrounded by rubber before extraction. This identification confirms the interpretation of ternary blend micrographs given by Thamm[6] and Salovey, Naderi, and Chompff.[8]

Experiments in which ternary blends were heated in the melt for various times show that particles grow in the melt and that the HDPE particles eventually become completely surrounded by PEP. An unmolded Banbury-mixed sample, which was made by mixing equal proportions of 85PP–15PEP and 85PP–15HDPE, contained small particles of the order of 0.2 μm in diameter [Fig. 4(a)]. After compression molding with 5 min of melt residence time, particles of the order of 1 μm in diameter were obtained [Fig. 1(c)], with further growth occurring at longer residence times [Fig. 4(b)]. Areal fraction data obtained from such

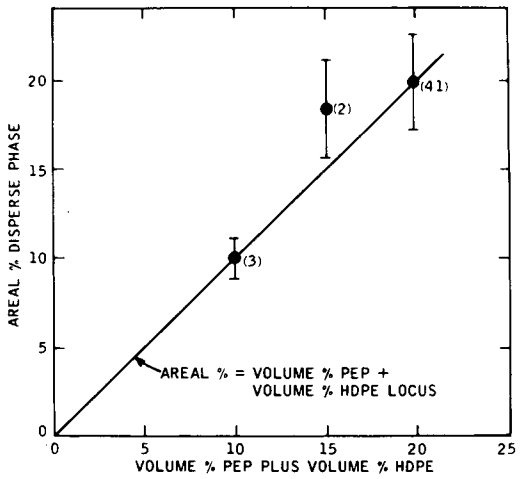

Fig. 3. Areal percent disperse phase in scanning electron micrographs of compression molded PP–PEP–HDPE blends of various composition. PP–PEP–HDPE blend compositions are 90:5:5, 85:7.5:7.5, and 80:10:10.

micrographs are summarized in Table II. The sum of the areal fractions of empty holes and partly filled holes was independent of melt residence time within experimental error. However, the areal fraction of empty holes increased with residence time, and the areal fraction of partly filled holes decreased correspondingly. These results are interpreted as follows. When PP-rich ternary blends are mixed, rubber and HDPE combine to form composite particles dispersed in PP. At short melt residence time, rubber does not completely surround the HDPE particles and HDPE is partly attached to the PP matrix. Upon subsequent extraction, the HDPE particles are retained in the partly empty cavity by the PP–HDPE attachments. At long melt residence times, however, the PP–HDPE attachments are displaced, and the HDPE particles become completely enveloped by rubber. When rubber is extracted from a cut surface of such a specimen, the insoluble but unattached HDPE particles are flushed away, leaving an empty hole.

The tendency for PEP to envelop HDPE, rather than vice versa, in a PP matrix is reasonable from interfacial energy considerations. If PP, PEP, and HDPE are completely insoluble, then the HDPE-within-PEP structure illustrated in Figure 5(a) will be thermodynamically favorable over a PEP-within-HDPE structure if $\gamma_{PP-PEP} < \gamma_{PP-HDPE}$, where γ is the interfacial energy. Helfand's theory for the interfacial energy of polymer pairs,[11] using solubility parameters estimated by the method of Krause,[12] indicates that this condition is indeed fulfilled. The growth of the particles in the melt, which is evident from Figure 4, results from the thermodynamic drive to reduce the interfacial area and interfacial energy of the system.

If PP, PEP, and HDPE formed a single phase at 200°C, the melt temperature of the above experiments, then the particle size observed at room temperature should be independent of melt residence time. Thus, the growth of particles which occurs upon annealing in the melt implies that the mixtures are incompatible in the melt.

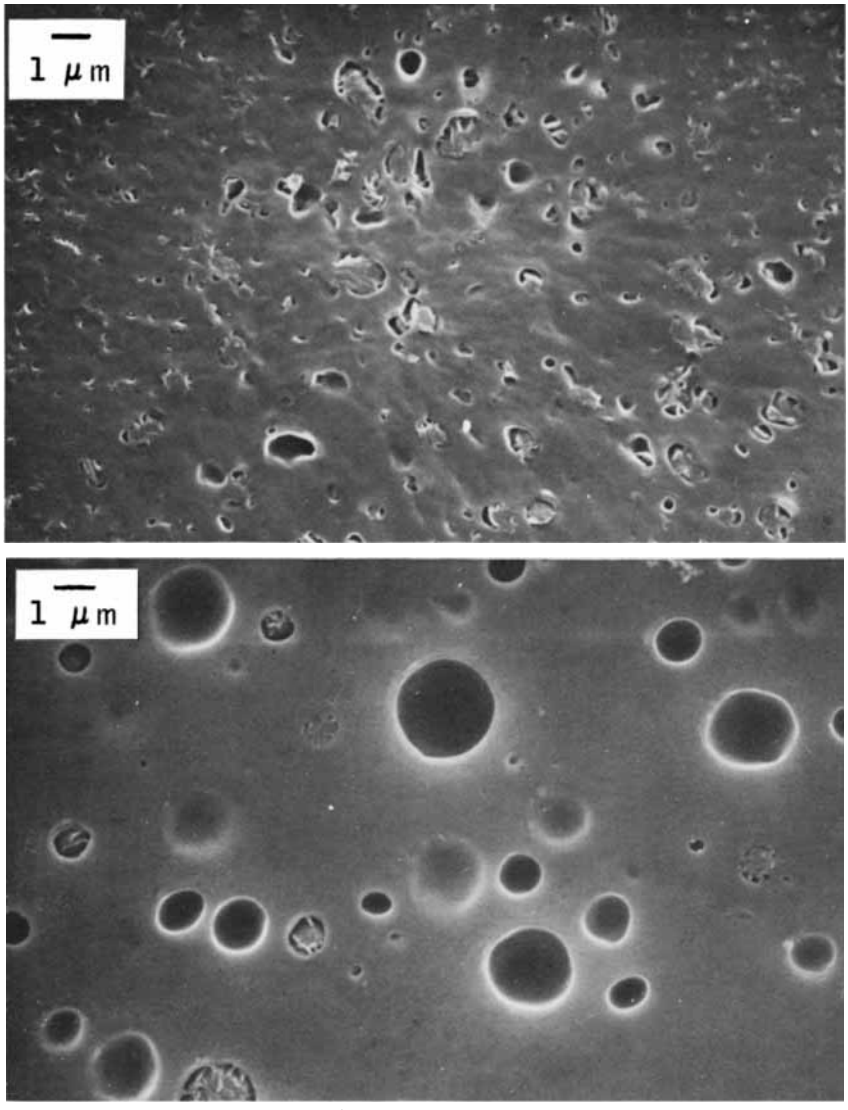

(a)

(b)

Fig. 4. Scanning electron micrographs showing effect of melt residence time on structure: (a) unmolded 85PP–7.5PEP–7.5HDPE blend made by intensive mixing of 50:50 mixture of 85PP–15PEP and 85PP–15HDPE; (b) same as (a) but compression molded with 80 min of melt residence time at 200°C.

A major departure from the structure depicted in Figure 5(a) for PP-rich ternary blends occurred only when PEP and HDPE were mixed together before PP addition. As shown in the Figure 6(a) micrograph, binary PEP–HDPE mixtures with an approximately 1:1 composition ratio formed an interpenetrating, cocontinuous structure similar to that observed in 70PP–30PEP blends by Kresge.[13] When premixed PEP–HDPE was mixed with PP, micrographs similar to that shown in Figure 6(b) were obtained. As illustrated schematically in Figure 5(b), the larger of the composite PEP–HDPE particles retained the interpenetrating structure existing in the PEP–HDPE blends before PP addition. Smaller particles in the distribution, on the other hand, tended toward the layered structure shown in Figure 5(a).

TABLE II
Increase of Empty Hole Concentration with Melt Resistance Time

Residence time in melt at 200°C, min	Areal percent, % Partly filled holes	Empty holes	Sum
5	12.1	9.1	21.2
20	5.5	15.0	20.5
80	4.3	15.7	20.0

Impact Strength of Ternary PP–PEP–HDPE Blends

Our findings on the structure of PP impact blends provide a basis for interpreting their impact properties. HDPE by itself is ineffective in toughening PP, presumably because the dispersed HDPE particles do not initiate crazes nor arrest crack growth as effectively as rubber particles. This behavior may be

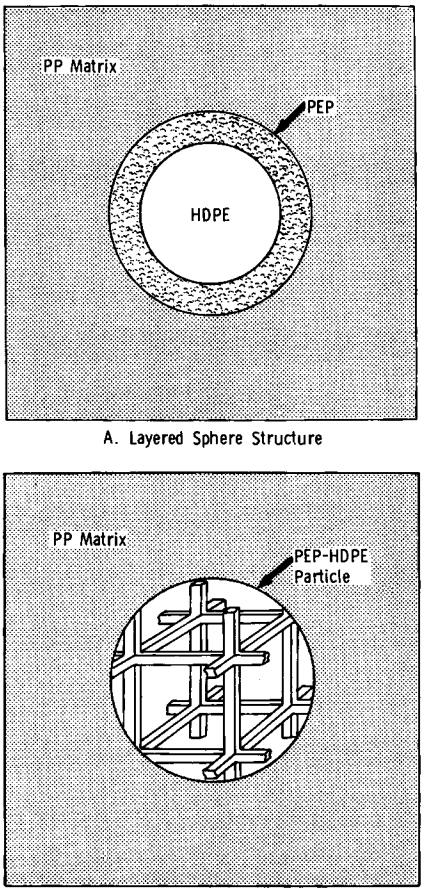

Fig. 5. Schematic illustrations of morphology of composite PEP–HDPE particles in PP-rich ternary blends: (a) layered particle with PEP shell around HDPE inclusion; (b) particle with interpenetrating PEP–HDPE structure. For purposes of clarity, the strands of the interpenetrating HDPE–PEP particle are not drawn to scale.

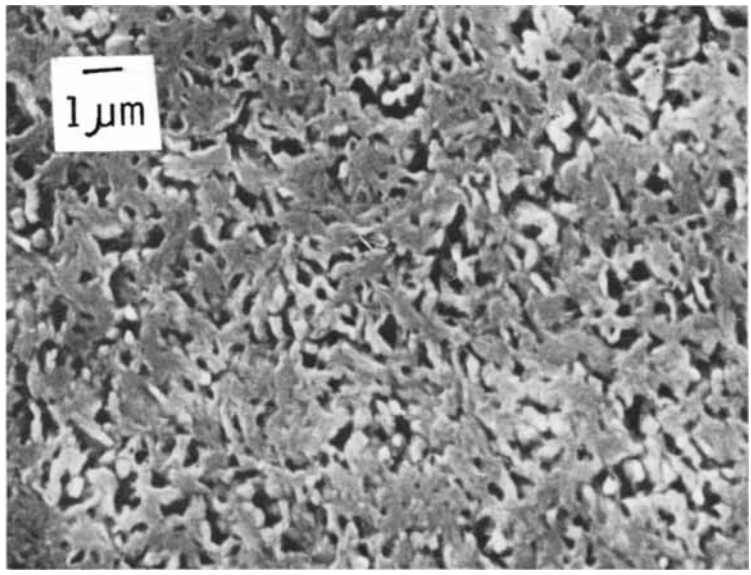

(a)

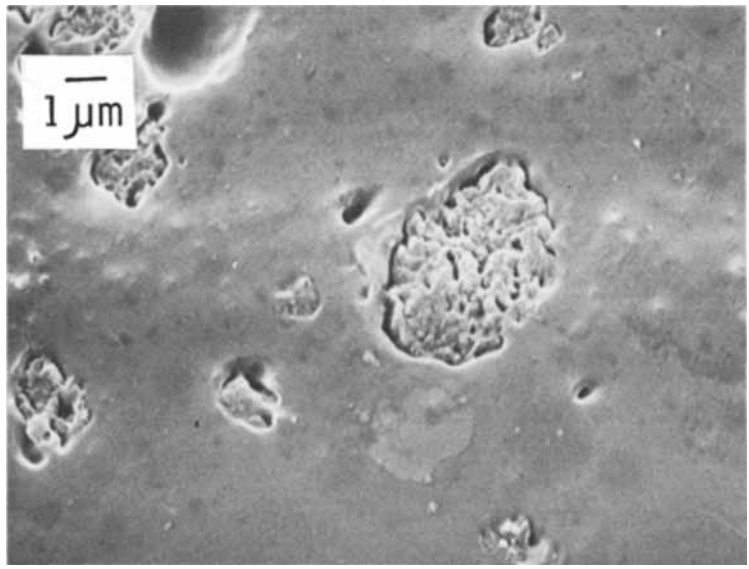

(b)

Fig. 6. (a) Scanning electron micrograph of compression-molded 50PEP–50HDPE sample prepared from intensively mixed blend. (b) Micrograph of compression-molded 80PP–10PEP–10HDPE sample made by adding PP to premixed 50PEP–50HDPE.

caused by poor PP–HDPE adhesion as well as by the nonrubberlike characteristics of HDPE. However, as illustrated in Figure 7, HDPE used in admixture with PEP is an effective toughening agent for PP.[14] In PP-rich blends, PEP rubber can be replaced by HDPE with but little loss of impact strength, provided, however, that HDPE constitutes no more than 50 vol % of the total impact additive. At a constant total additive level, increasing the HDPE volume fraction beyond 50% causes a sharp decline in toughness. These observations can be explained in terms of the morphology of ternary blends and stress distributions around composite particles in a matrix. As shown above, when small quantities

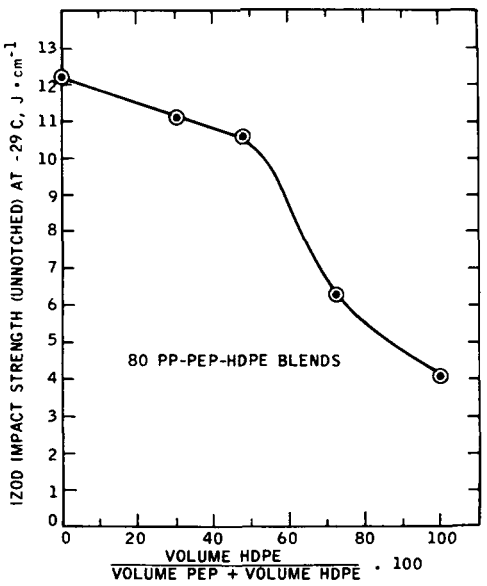

Fig. 7. Impact strength of PP–PEP–HDPE blends with 80 vol % PP and varying PEP and HDPE concentration.

of PEP and HDPE are mixed with PP, they combine to yield composite particles with rubber tending to form a shell around an HDPE inclusion. Theoretical calculations by Ricco, Pavan, and Danusso show that the stress distribution around a spherical rubber particle is almost unaffected by the presence of a hard inclusion so long as the volume fraction of inclusion is less than 60–70%.[15] Thus, at modest HDPE loadings, the composite rubber–PP particle should have the craze initiation characteristics of a rubber particle with attendant high-impact strength. At higher HDPE loadings, the composite particles gradually acquire the presumably poor craze initiation and crack arrest characteristics of HDPE, with consequent loss of impact strength. Alternatively, the poor impact strength of PP-rich ternary blends having high HDPE:rubber ratios may be caused by incomplete envelopment of HDPE inclusions, with resulting poor adhesion between particle and matrix. If HDPE tended to form a shell around a rubber inclusion, rather than vice versa, all PP-rich ternary blends would have poor toughness.

We are not aware of calculations of stress distributions around spheres having interpenetrating hard and soft phases. However, the impact strength of ternary blends having the interpenetrating disperse phase structure was identical to that of blends having the layered disperse phase structure (see below), so we assume that the above considerations also apply qualitatively to this structure.

The size of composite PEP–HDPE particles in ternary PP–PEP–HDPE also has a strong effect on impact strength. Impact strength data on 80PP–10.7PEP–9.3HDPE blends having different particle sizes are listed in Table I. Blends 3 and 4 were prepared by mixing a premixed PEP–HDPE blend with PP at different conditions in an extruder. The well-mixed sample, blend 3, with a number-average diameter $\bar{d}_1$ of 0.64 μm, had much greater impact strength than the poorly mixed sample, blend 4, with $\bar{d}_1$ equal to 2.1 μm. Additional data obtained on both compression-molded and injection-molded samples showed

that impact strength increased as particle size decreased over this size range. Higher impact strength would presumably be obtained for particle diameters less than 0.6 μm. However, access to test specimens with such small particle size was limited by particle growth during molding of the test pieces.

The optimum particle diameter for toughening of brittle plastics by rubber addition ranges from ~0.1 to ~3 μm.[16] The optimum size falls at the low end of the range for relatively ductile polymers such as PVC that deform mainly by shear yielding and at the high end of the range for relatively brittle polymers such as polystyrene that deform mainly by crazing.[17] PP at room temperature is a relatively ductile material that deforms mainly by shear yielding,[18] so the optimum particle diameter should fall at the low end of the range. Our finding that the optimum diameter for PP toughening is less than or equal to 0.6 μm is consistent with this expectation.

Flexural Modulus of Ternary Blends

At constant composition, the modulus of ternary blends was independent of particle size to within experimental error. However, as shown below, modulus was mildly dependent on the internal structure of the composite PEP–HDPE particles. Flexural modulus and impact strength of 76PP–12PEP–12HDPE and 86PP–6PEP–6HDPE blends prepared by two different mixing sequences are compared in Table III. Blends A and C were produced by premixing PEP and HDPE before PP addition, and the larger particles in the mixture had the interpenetrating particle structure depicted in Figure 5(b). Blends B and D, on the other hand, were made by mixing PP–PEP with PP–HDPE, and they tended toward the layered structure depicted in Figure 5(a). Blends having the same composition prepared by the two mixing procedures had equal impact strengths within the precision of the tests. However, blends made using premixed PEP–HDPE added to PP had significantly higher flexural modulus than blends having the same composition made by the other mixing procedure.

TABLE III
Effect of Blending Sequences on Mechanical Properties

	Flexural modulus at 23°C, MPa	Impact strength[a] Notched Izod at 23°C, J/cm	Unnotched Izod at −28°C, J/cm	Falling weight, J
88PP-6PEP-6HDPE Blends				
A. PEP and HDPE premixed before PP addition	1340	0.5	7.0	1.4
B. PP–PEP mixed with PP–HDPE	1290	0.5	7.5	1.6
76PP-12PEP-12HDPE Blends				
C. PEP and HDPE premixed before PP addition	1060	0.9	14.4	12.9
D. PP–PEP mixed with PP–HDPE	990	1.0	15.5	12.6
Standard deviation of test	12	0.1	0.9	0.3 at 1.5 level 0.9 at 12 level

[a] Injection-molded samples.

The observed difference in modulus of the two types of blends can be explained using Kerner's theory for the modulus of composites containing spherical inclusions.[19] According to this theory, the modulus of the composite, at a given matrix modulus and volume fraction of spheres, increases as the modulus of the included spheres increases. In our case, the spheres are themselves composites of PEP and HDPE having the structures shown in Figures 5(a) and 5(b). Gent's theory for the modulus of interpenetrating phases[20] was used to estimate the modulus of interpenetrating 50PEP–50HDPE particles, and Matonis and Small's calculations of the modulus of layered rubber particles containing hard inclusions[21] were used to estimate the modulus of layered 50PEP–50HDPE particles. Kerner's theory then leads to the conclusion that ternary blends with the interpenetrating PEP–HDPE structure have a greater modulus than those with the layered PEP–HDPE structure. The calculated difference of the modulus of the two types of structures for 76PP–12PEP–12HDPE and 86PP–6PEP–6HDPE blends, 74 and 43 MPa, respectively, compares favorably with the experimentally measured differences, 70 and 50 MPa, respectively.

Advantages and Limitations of the Method for Examining Blend Structure

The above results demonstrate the utility of our method for examining the morphology of PP–PEP–HDPE blends. It is important to emphasize that the method is a quantitative method for examining blend structure and that some of our conclusions could not have been obtained by a qualitative technique. Examination of a microtome surface rather than a fracture surface is preferred because features on a fracture surface may not be representative of the bulk structure of the composite.

On the other hand, our method suffers several limitations. Securing a microtome surface takes more time, skill, and equipment than securing a fracture surface. Experience has shown that our method is not so useful when rubber concentration is very low, less than about 1%. Furthermore, the method is not applicable when the rubber is crosslinked because it cannot then be extracted from the surface. Chemical etching with chromic acid can then be used to selectively attack the rubber on the surface, but micrographs so obtained have been less revealing than micrographs presented in this paper.

If a rubber can be suitably stained and if the highest possible resolution is desired, then the examination of stained thin sections by TEM is preferred over the SEM method. Cutting of sections suitable for TEM examination, however, requires greater skill than cutting a face on a block for SEM inspection. Thin sections are also distorted so that shapes of particles cannot be accurately determined by the TEM method.[2]

Effect of Rubber Type on Impact Strength of Plastic–Rubber Blends

The preceding experiments show that PEP is an excellent rubber for toughening PP. Other rubbers might also be considered for this purpose, and a theory which correctly predicts if a specific rubber would be a good toughening additive for a specific brittle polymer would be very useful. It has been suggested, among other requirements, that rubber addition to a plastic will improve toughness only

if the two components form two phases and if there is good adhesion between the two phases.[2,22] We have attempted to place these two requirements on a more quantitative basis by the following considerations. Phase separation of polymer mixtures can be treated using Scott's extension of the Flory–Huggins theory of polymer solutions to polymer mixtures.[23] For polymer pairs where there are no specific interactions such as hydrogen bonding or strong dipolar forces, phase separation will occur only if the absolute value of the difference between solubility parameters of the two components, $|\delta_1 - \delta_2|$, is sufficiently large. Following Krause[12] and assuming a molecular weight of 10^5 for each component, the critical value of the solubility parameter difference, $|\delta_1 - \delta_2|_c$, which must be exceeded for phase separation to occur at various compositions at 25°C, is shown in Table IV. If phase separation is to occur at low rubber contents of about 5–10%, then $|\delta_1 - \delta_2|$ must be greater than 0.2 $(\text{cal/cm}^3)^{1/2}$.

We consider adhesion between polymer pairs with the aid of Helfand's theory for the thickness of the interface between two polymer phases.[11] According to the theory, interfacial thickness increases as $|\delta_1 - \delta_2|$ decreases. Interfacial thicknesses calculated as a function of $|\delta_1 - \delta_2|$ are listed in Table IV. Here we see, for example, that a polymer pair having a large solubility parameter difference of 1.7 will have a small interfacial thickness of 0.7 nm, whereas a small solubility parameter difference of 0.12 causes a large interfacial thickness of 10 nm. We now introduce the hypothesis that good adhesion requires physical entanglement between the two kinds of molecules in the interface. Taking the number of chain bonds between entanglement points[24] to be a typical value equal to 500, a 0.15-nm bond distance, and assuming freely jointed bonds, the root-mean-square distance between entanglements is $0.15 \times 500^{1/2}$ nm, i.e., 3.3 nm. This approach thus leads to the conclusion that the interfacial thickness should be greater than 3 nm for good adhesion, which, from Table IV, requires that $|\delta_1 - \delta_2| < \sim 0.4$.

There are few published data to test these suggested conditions for impact improvement upon rubber addition to a plastic, i.e., $|\delta_1 - \delta_2| > 0.2$ for phase separation and $|\delta_1 - \delta_2| < 0.4$ for good adhesion. Testing of these criteria is also

TABLE IV
Calculated Relations Between Composition of Binary Blends, Critical Difference in Solubility Parameters, and Interfacial Thickness

Concentration of minor component, vol %	Critical Difference in Solubility Parameters for Phase Separation $\lvert\delta_1 - \delta_2\rvert_c$,[a] $(\text{cal/cm}^3)^{1/2}$	Interfacial Thickness Corresponding to $\lvert\delta_1 - \delta_2\rvert_c$, nm
30	0.12	10.2
20	0.13	9.3
10	0.18	6.8
5	0.24	5.1
1	0.55	2.3
0.5	0.77	1.6
0.1	1.7	0.7

[a] Assumes molecular weights of 10^5, temperature of 25°C.

confounded by the fact that solubility parameters of polymers measured by various methods differ substantially. As recommended by Krause, we have therefore used calculated solubility parameters based on Hoy's group contribution table[25] to test the theory. Table V gives impact strength values obtained on 87% poly(vinyl chloride) (PVC)–13% rubber blends by Matsuo et al. The rubbers tested included poly(butadiene-co-acrylonitrile) of varying composition, PEP, and poly(styrene-co-butadiene). Calculated solubility parameters for the various polymers are listed in the table, together with PVC–rubber solubility parameter differences, $|\delta_{PVC} - \delta_R|$. Focusing attention on the PVC–poly(butadiene-co-acrylonitrile) system, $|\delta_{PVC} - \delta_R|$ increases systematically from 0.1 to 1.3 as the acrylonitrile content of the copolymer decreases from 40% to 0%. By our analysis, the impact strength of the blend made using 60% butadiene–40% acrylonitrile rubber should be poor because of failure to form two phases, whereas the impact strength of the blend made using 100% butadiene–0% acrylonitrile rubber should be poor because of poor adhesion. Additionally, impact strength should pass through a maximum at an intermediate composition, specifically at a 70% butadiene–30% acrylonitrile composition, for which $|\delta_{PVC} - \delta_R| = 0.3$. The experimental data show that impact strength indeed passes through a maximum, albeit at an 80% butadiene–20% acrylonitrile composition rather than at the predicted 70:30 composition. Furthermore, investigations have shown that PVC and poly(butadiene-co-acrylonitrile) rubber with 30–40% acrylonitrile form a single-phase solution, whereas PVC and polybutadiene are incompatible.[27] Finally, as predicted by the theory, ethylene–propylene copolymers and styrene–butadiene rubbers are poor toughening agents for PVC. Overall, considering the simplicity of the theory, the uncertainty in solubility parameters and the fact that other factors can also affect impact strength, the experimental results and the predictions of the model are in satisfactory agreement.

The preceding model is presented only as a rough guide for screening rubbers as possible toughening agents for brittle plastics. Solubility parameters for PP and PEP containing 50 mol % ethylene are 7.38 and 7.62, respectively, yielding $|\delta_{PP} - \delta_R| = 0.24$. PEP is thus predicted to be a good impact modifier for PP. This prediction is in accord with the experimental results discussed above.

TABLE V
Relation Between Solubility Parameters and Impact Strength of Rubber-Reinforced PVC

Rubber	Rubber solubility parameter δ_R, $(cal/cm^3)^{1/2}$	Solubility parameter difference $\lvert\delta_{PVC} - \delta_R\rvert$,[a] $(cal/cm^3)^{1/2}$	Charpy impact strength of 87PVC–13 rubber blends at 20°C, J/cm
Butadiene–nitrile rubbers			
100 Butadiene–0 acrylonitrile	8.24	1.3	3
80 Butadiene–20 acrylonitrile	8.84	0.7	27
70 Butadiene–30 acrylonitrile	9.22	0.3	7
60 Butadiene–40 acrylonitrile	9.60	0.1	2
Ethylene–propylene rubber (50:50)	7.68	1.7	3
Styrene–butadiene rubber (25:75)	8.52	1.0	4

[a] Solubility parameter of PVC is 9.54 $(cal/cm^3)^{1/2}$.

CONCLUSIONS

The preceding results show that the examination of solvent-etched microtomed surfaces cut at low temperatures is a valid method for examining the state of dispersion of PEP and HDPE in PP-rich blends. When small amounts of PEP and HDPE are added to PP, the two additives combine to form composite PEP–HDPE particles in a PP matrix. The effectiveness of HDPE in improving impact strength when used in admixture with PEP is a consequence of the tendency for the rubber to form a shell around an HDPE inclusion. This characteristic layered morphology can be partially circumvented by premixing PEP and HDPE before PP addition. In this event, the composite PEP–HDPE particles tend to have an interpenetrating structure. Which of these two limiting structures prevails has little affect on impact strength. However, blends with interpenetrating PEP–HDPE particles have modestly higher modulus than blends with layered particles.

The size of the composite PEP–HDPE particles in PP-rich blends has a strong affect on impact strength. Impact strength increases as particle size decreases to 0.6 μm in diameter, the smallest diameter observed in molded objects. Smaller particles are readily achieved in intensive mixing devices. However, rapid particle growth occurs in the melt during molding, and particle sizes less than 0.6 μm are not easily achieved in molded objects. Inhibition of particle growth by crosslinking or by addition of block copolymer molecules is an obvious approach to obtaining and maintaining an excellent dispersion of impact modifiers.

Finally, the suggested requirement that the $|\delta_1 - \delta_2|$ be approximately equal to 0.3 to achieve phase separation and good rubber–matrix adhesion appears to be a useful criterion for screening rubbers to toughen a brittle plastic.

The authors gratefully acknowledge the experimental assistance of H. Tarski, P. Casey, and R. Stockton.

References

1. Exxon Chemical Co. Brochure, *Exxon Elastomers for Polyolefin Modification*, 1975.
2. C. B. Bucknall, *Toughened Plastics*, Applied Science Publishers, London, 1977, p. 39.
3. K. Kato, *J. Electron Microsc.*, **14,** 220 (1965).
4. K. Kato, *Polym. Eng. Sci.*, **7,** 38 (1967).
5. K. Kato, *Kolloid-Z. Z. Polym.*, **220,** 24 (1967).
6. R. C. Thamm, *Rubber Chem. Technol.*, **50,** 24 (1977).
7. W. M. Speri and G. R. Patrick, *Polym. Eng. Sci.*, **15,** 668 (1975).
8. R. W. Salovey, J. Ho, A. Naderi, and A. J. Chompff, *Polym. Prep. Am. Chem. Soc. Div. Polym. Chem.*, **20,** 516 (1979).
9. G. Herdan, *Small Particle Statistics*, Academic, New York, 1960, p. 237.
10. J. Karger-Kocsis, A. Kallo, A. Szafner, G. Bodor, and Z. Senyei, *Polymer*, **20,** 37 (1979).
11. E. Helfand and Y. Tagami, *J. Polym. Sci.*, **9B,** 741 (1971).
12. S. Krause, *J. Macromol. Sci. Rev. Macromol. Chem.*, **C7**(2), 251 (1972).
13. E. N. Kresge, in *Polymer Blends*, Vol. 2, D. Paul and S. Newman, Eds., Academic, New York, 1978, p. 293.
14. R. L. Hull, unpublished work.
15. T. Ricco, A. Pavan, and F. Danusso, *Polym. Eng. Sci.*, **18,** 774 (1978).
16. Reference 2, p. 185.
17. Reference 2, p. 208.
18. F. C. Stehling, unpublished work.
19. E. H. Kerner, *Proc. Phys. Soc. London*, **69B,** 802, 808 (1956).
20. A. N. Gent and A. G. Thomas, *Rubber Chem. Technol.*, **36,** 597 (1963).

21. V. A. Matonis and N. C. Small, *Polym. Eng. Sci.*, **9,** 90 (1969).
22. S. L. Rosen, Sixth Akron Summit Polymer Conference, Sept. 11, 1975, Akron, Ohio.
23. R. L. Scott, *J. Chem. Phys.*, **17,** 279 (1949).
24. R. Porter and J. Johnson, *Chem. Rev.*, **66,** 1 (1966).
25. K. L. Hoy, *J. Paint Technol.*, **42,** 76 (1970).
26. M. Matsuo, A. Veda, and Y. Kondo, *Polym. Eng. Sci.*, **10,** 253 (1970).
27. S. Krause, in *Polymer Blends*, D. R. Paul and S. Newman, Eds., Academic, New York, 1978, pp. 65–68.

Received December 9, 1980
Accepted January 22, 1981